Publications of the Astronomical Society of the Pacific
104: 592–596, 1992 July

A Deconvolution Technique for *Hubble Space Telescope* FGS Fringe Analysis[1]

JOHN L. HERSHEY

Astronomy Programs, Computer Sciences Corporation, Space Telescope Science Institute, 3700 San Martin Drive, Baltimore, Maryland 21218
Electronic mail: hershey@scivax.stsci.edu

Received 1992 March 11; accepted 1992 April 21

ABSTRACT. A technique has been developed for directly transforming interferometer fringe visibility functions ("*S* curves") from the *Hubble Space Telescope* (*HST*) fine guidance sensors (FGSs) into intensity profiles of the program object. In a process analogous to Fourier transform image deconvolution, an *S* curve from a double star yields a pair of narrow profiles containing information on the separation (in one coordinate), and relative brightness of the two stars. The procedure has yielded high internal precision for the separation and relative brightness in tests with *HST* data. Simulations indicate that it can also deconvolve *S* curves from multiple stars or continuous intensity distributions such as resolvable stellar or extragalactic objects. Similar deconvolution analyses may be useful in other types of interferometry.

1. INTRODUCTION

The three fine guidance sensors (FGSs) on the *Hubble Space Telescope* (*HST*) can be used in an interferometric mode to scan across a target and generate interference fringes simultaneously in two orthogonal coordinates. Many details of this process are described in the current edition of the *Hubble Space Telescope Fine Guidance Sensors Instrument Handbook* (FGS Instrument Team, 1992) available from the Space Telescope Science Institute. FGS observations of some Hyades stars have been analyzed by Franz et al. (1992) and much information is provided there on the acquisition of data, the generation of *S* curves from the observational data obtained by the FGSs, and plots of various *S* curves.

The analysis by Franz et al. (1992) was carried out with the purpose of searching for duplicity in the program stars. Double-star *S* curves were synthesized from a reference *S* curve using linear superposition. The separations and relative amplitudes were varied and a grid of combinations was explored for best fit. A binary of 180 milliarcsec (mas) separation was clearly detected and measured.

After working on FGS data extraction and unrelated experimentation with image deconvolution, it occurred to me to try deconvolving the *S* curves back to their source profiles using the convolution relation for Fourier transforms. Some results of this procedure, applied to observational data, are reported here.

2. DECONVOLUTION RELATIONS FOR *S*-CURVE ANALYSIS

The Fourier transform relation representing a convolution is given by Press et al. (1986), p. 383, and may be expressed verbally for two functions *A* and *B* as: the product of the Fourier transform of *A* and the Fourier transform of *B* equals the Fourier transform of the convolution of *A* and *B*. Regarding *A* as the "signal" function and *B* as the "convolving" or "response" function the relation may be written for image convolution as

FT(source intensity distribution) × FT(PSF)
= FT(blurred image).

[Multiplication or division for Fourier transforms (FTs) is assumed hereinafter to be multiplication or division of complex vectors.] In this application the blurred image and the point spread function (PSF) are observed and thus known. The source intensity distribution is unknown at the desired resolution and therefore can be determined, in principle, by an inverse Fourier transform of the quotient of the Fourier transforms of the observed functions.

The convolution relation for *S*-curve analysis is assumed to be

FT(source intensity distribution) × FT(*S* curve of a single star) = FT(observed *S* curve).

Abbreviating the function names above and rearranging, the mathematical relation for restoration of the source distribution becomes

Source intensity distribution = inverse FT [FT(observed *S* curve)/FT(*S* curve of a single star)].

The source distribution for a single star may be thought of ideally as a delta function. For a double-star *S* curve the deconvolution ideally would yield two scaled delta functions whose separation and areas would represent the separation (in one coordinate), and relative brightness of the pair. In practice the results are not ideal delta functions but "spikes" or image profiles whose lower limit of width is primarily a result of photon noise in the data, but guiding error of the telescope may contribute very small and very low-frequency noise components.

The significant Fourier components of the *S* curve are at the low-frequency end because the fringe is primarily a

[1]Based on observations with the NASA/ESA *Hubble Space Telescope*, obtained at the Space Telescope Science Institute, which is operated by the Association of Universities for Research in Astronomy, Inc., under NASA Contract No. NAS5-26555.

single oscillation of the visibility function in a scan. As a result, filtering of the low-signal-to-noise region is simplified to suppressing all but the low end of the Fourier spectrum. In contrast, image deconvolution often involves image features with spectral components throughout the entire frequency range, presenting a complicated filtering problem. Furthermore in the case of the *S* curves the noise is essentially all photon noise which has constant power with frequency. (The *S* curve runs both positive and negative because it is the difference of two PMT outputs.) For a fringe formed from discrete sources, well above limiting brightness, there should be little chance for cases where a unique deconvolution solution does not exist. Since the FGS data is taken with constant step size, fast Fourier transforms (FFTs) may be used without special data preparation.

The deconvolution was done with the Interactive Data Language ("IDL") (a registered trademark of Research Systems, Inc.), a computational language in which FFT operations are part of the language. Operations on vectors need no indexing if the full vector is used. Complex multiplication and division are implicit in the language for complex vectors. Three short FFT statements, a division statement, and a few lines for filtering do all of the mathematical operations for the deconvolution and are performed in a few seconds.

3. DECONVOLUTION OF *HST S* CURVES

The deconvolution method was applied to the same data analyzed by Franz et al. (1992). The observations were part of the *HST* "Science Assessment Observations" for preliminary observational tests of *HST* instruments. The *HST* proposal originated with the ST Astrometry Team. The observations were made in late 1990 and the stars observed are listed in Table 1 of Franz et al. (1992).

Ten sequential scans in alternating directions had been obtained for all stars. For the analysis and the figures shown here, mean *S* curves were formed by shifting the individual scans to find the point of minimum difference and then averaging together all individual scans not obviously distorted by telescope motion. The step size in a scan is determined by commands telemetered to the FGS. A nominal scale of 100 data points = 149 mas was adopted for the data used here.

The deconvolution requires a "reference" *S* curve of a single star with as little noise as possible, from the same FGS unit and FGS field-of-view location as the "unknown" sources so that it has the same details of fringe shape. A mean of *S* curves for three bright single stars was used for the reference *S* curves in the work described here. The three stars were checked for evidence of duplicity in many solutions with combinations of reference and unknown curves. The *S* curve in the interferometer *X* coordinate for the double star (star M in Franz et al. 1992) is shown in Fig. 1.

The sequence of mathematical operations is best understood with a series of figures. The absolute value of the FFT of the *S* curve in Fig. 1 is shown in Fig. 2 and represents the amplitudes of the Fourier components. The absolute value is the square root of the sum of the squares of imaginary and real components (or square root of the power spectrum). Frequency increases positively from the left to the middle of the plot and negative frequencies go increasingly negative from the right. (The FFT in this form is symmetrical, with one half redundant.) Clearly the information for the *S* curve is at low frequency, near each end of the FFT plots, and the majority of the length of the spectrum is noise. The FFTs of double- and single-star *S* curves have this same general appearance.

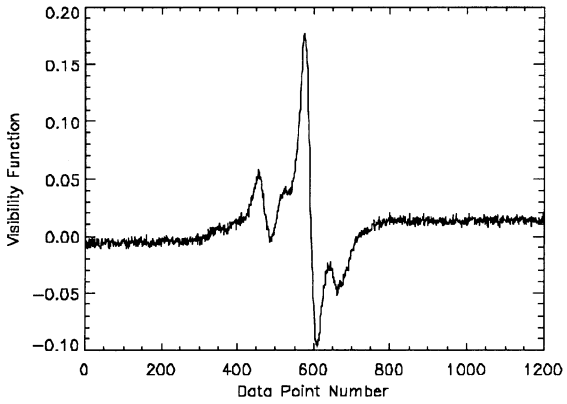

FIG. 1—The *S* curve for star M, the double star in Franz et al. (1992). Nominal scale for the abscissa is 149 milliarcsec = 100 points. The *S* curve visibility function in the ordinate is defined in the references.

The absolute value of the quotient of the FFT of the unknown divided by the reference FFT is shown in Fig. 3. Again the ends clearly carry the information but the noise throughout most of the FFT is greatly accentuated by the division of the two FFTs. An inverse FFT of this quotient, without filtering, would yield only noise.

With a filter function that passes only each end of the quotient vector, an inverse FFT is carried out on the quotient and the deconvolved star profile is generated. For

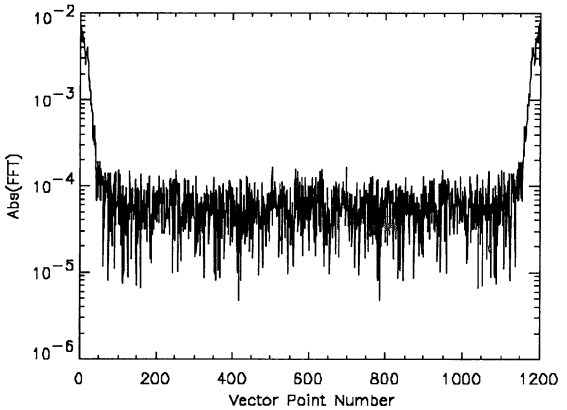

FIG. 2—The absolute value of the FFT of the *S* curve in Fig. 1. The ordinate is the square root of the sum of the squares of the real and imaginary parts of the FFT. On the abscissa zero frequency is at the left with positive frequencies increasing toward the center of the plot, and negative frequencies beginning at the right. Frequency at the center is ±1/2 cycle per point and ±1/1200 cycles per point at the first positive or negative point. (In this form the FFT is symmetrical and one-half is redundant.)

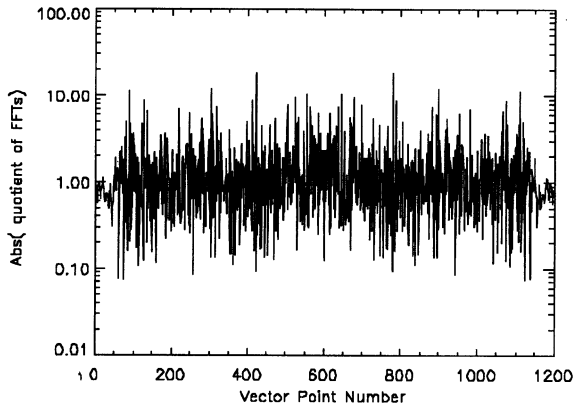

FIG. 3—The absolute value of the quotient of the FFT in Fig. 2 and the FFT of a single star. The comments in Fig. 2 apply.

plotting deconvolved profiles it is helpful to exchange the halves so that the star images are not split at each end but appear in the center of the plot. With deconvolution of the unknown curve in Fig. 1 a double-star profile emerges (Fig. 4).

The areas under the profiles represent the relative energy from each star. However, the base widths of the profiles are set by the filter and so are essentially equal. Consequently the heights of the profiles also closely represent the relative brightness.

For the Y coordinate of the same star a single-star profile emerges (Fig. 5). In agreement with Franz et al. (1992), it was found that star M has its companion situated very close to the X axis of the interferometer, yielding an apparently single profile on the Y axis. (The area of the Y profile does not necessarily equal the two X profiles since the two coordinates are served by separated optics and photomultipliers, but the difference could be calibrated.)

After much experimentation with various filter functions it was found that a filter which leaves some points unchanged at each end and then drops off exponentially toward higher frequencies, worked very well. For the stars analyzed here, typically ten points at the ends were left unchanged and a filter factor of $\exp[-(n-10)/15]$ was applied to the remainder of the quotient vector. A proper filter is a function of many parameters such as the number of points in the data vector, brightness of the star, and quality of the reference S curve. The choice of the filter width is a trade-off between increasing noise and narrower profiles in the direction of wider filter transmission and smooth but broadened profiles as the filter is changed in the narrower direction.

A Wiener filter (Press et al. 1986, p. 417ff) includes higher frequencies and a sharper cutoff than used here. The filter would be approximately $\exp[-(n-50)/6]$, but depends on some interpretation of the signal and noise functions. The result in the deconvolution is a narrower spike but large oscillations in the background. For the well-resolved double in Fig. 4, the sharper spikes are not needed and the higher frequency oscillations in the background are suppressed by a filter with a lower frequency cutoff. Filters reaching to and above the Wiener frequency cutoff were used in searching for duplicity in other profiles.

The effects of a filter can be directly seen by deconvolving an S curve against itself. With no filter a nearly perfect delta function is returned, limited only by numerical processes. With a filter of the same shape as used in the deconvolution of the unknown curves, the width of the profile and small oscillations resulting only from the filter are revealed.

For a quantitative measure of the internal precision of the deconvolution method, the ten individual X scans of star M in Franz et al. (1992) were separately deconvolved using the three-star mean reference curve. A simultaneous differential correction solution for center, width, and area coefficient for each of two Gaussians and a constant was made on each of the ten double profiles (all similar to Fig. 4 but noisier). The magnitude difference, as represented by the area of the profiles, had a standard deviation of 0.26 mag or 0.08 in the mean and the separations had a standard deviation of 6 mas or 2 mas in the mean. Similarly an experiment deconvolving the mean S curve for star M against four different bright stars as reference curves yielded an error of 0.04 mag and 0.5 mas for the separation in the mean of four. Using the deconvolution of the mean

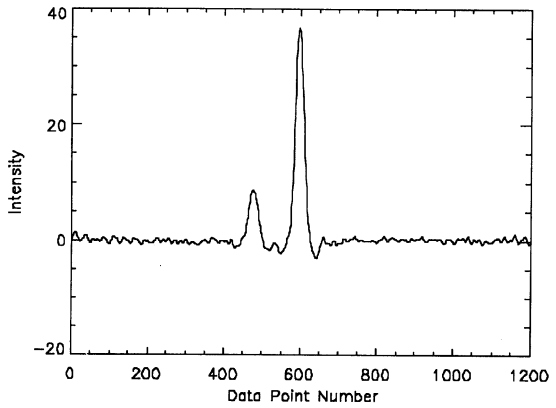

FIG. 4—Deconvolution for the S curve in Fig. 1. The abscissa scale remains the same as in Fig. 1. The ordinate is relative intensity and has not been calibrated in energy units.

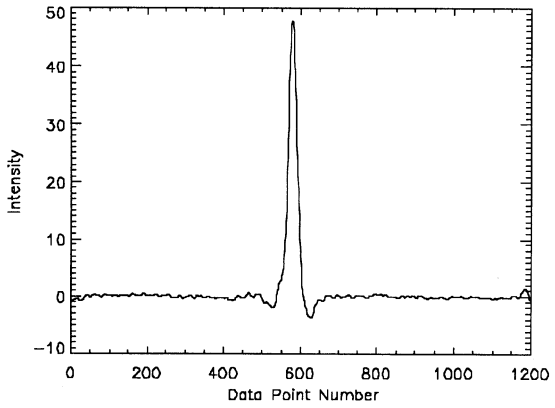

FIG. 5—The deconvolution for star M in the Y coordinate. The comments in the Fig. 1 and 4 legends apply.

curve for the double star, the resulting magnitude difference is 1.47 ± 0.09 and the separation is 181 ± 2 mas for the X direction, in agreement with Franz et al. (1992). Calibrations of the FGS scale may affect this value for the separation.

The errors cited above are, of course, strictly internal. More rigorous processing of the raw data might improve the above errors slightly. In particular no attempt was made to correct the individual scans for telescope jitter as sensed by the two guiding FGSs. Much more data will be needed to test the external and systematic errors of the entire process of observing and analysis. All of the Hyades data were processed and deconvolved, but no other significant evidence of duplicity was found, again in agreement with Franz et al. (1992). Special effort was made to resolve the Y coordinate for star M by fitting the deconvolved profile with overlapping Gaussians, by deconvolving the profile with other profiles run with the same filter, and by comparing profile widths, but no significant evidence of duplicity emerged.

HST data had also been taken for the visual binary ADS 11300 (Franz et al. 1991) when it was near periastron. A deconvolution easily separated the pair in the X direction at 55 mas in agreement with the curve fitting technique in the above reference. However, the profile and background were degraded by lack of a good reference profile.

4. SIMULATION EXPERIMENTS

Simulations were carried out for limiting detection capability for double-star separations. An observed single-star S curve was shifted and added to itself to simulate a close double. Using a different star for the reference curve, and filters including higher Fourier frequencies, separations of 30 mas show clearly as a double spike for equal magnitudes, and a difference of 1.5 mag was also clearly detectable visually at this separation. Smaller separations may well be reliably detected by fits of overlapping Gaussians or profile width comparisons.

Deconvolutions were also carried out for simulated multiple stars. The S curve resulting from shifting, adding, and scaling an S curve seven times forms a complicated S curve. Using the S curve from which the copies were generated as the reference curve, seven spikes emerge from the deconvolution with heights proportional to the amplitudes of the respective input S-curve components (Fig. 6).

The simulation was extended to a continuous source intensity distribution by adding and shifting 65 scaled copies of an S curve. The amplitudes increased linearly on the left, jumped to a flat top, and were followed by an exponential drop on the right. The deconvolution reveals a function with this same asymmetrical shape in Fig. 7. The input amplitudes in the simulations were normalized to sum to unity, causing the total area under the curves to remain constant. Figures 6 and 7 show little noise because the same single-star S curve was used for both the synthesis and the deconvolution canceling the observational noise below the filter limit.

For real data the restored continuous profile would represent the integrated intensity along a line perpendicular to the direction of the scan. It is analogous to a slit scan of the source image. In this view the "slit" is 5 arcsec long, which is the width of the square aperture in the image plane of the FGS, and the "width" of the slit is the single-star profile width determined by the FFT filter.

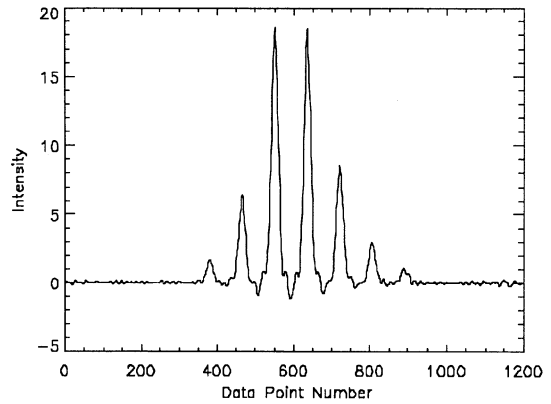

FIG. 6—A deconvolution for an S curve synthesized from seven shifts and amplitude scalings. The input S-curve amplitudes followed the same envelope and normalization described in Fig. 7.

5. CONCLUSIONS

Testing on more observational data will be necessary to show how the precision of the deconvolution technique compares with the curve fitting techniques. The deconvolution approach is certainly a much faster, more direct, and a more visual method. It could provide good starting points for the curve fitting process as well as independent checks on the results. For multiple stars, curve fitting would become computationally impractical and very difficult for continuous source distributions if their profiles were not elementary in shape.

The stars analyzed here from Franz et al. (1992) ranged from magnitude 8–12 (after adding 5 mag of neutral filtering in some cases). Deconvolutions of a few single-scan curves at magnitude 15 from another observation series

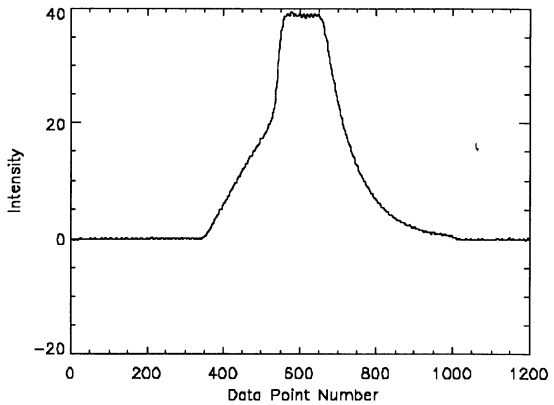

FIG. 7—A deconvolution for an S curve synthesized from 65 shifts and amplitude scalings. The envelope of the scalings first increased linearly then jumped to a flat top followed by an exponential decline. The amplitude scaling coefficients were normalized to sum to unity.

yielded strong profiles, indicating that much fainter stars should be amenable to deconvolution. The dependence of internal error on magnitude and the magnitude limit for deconvolution of the *S* curves from the FGSs have not yet been explored for lack of data.

Various enhancements for the method could be used. Further work, with theoretically formed filter functions may yield some improvement, especially for fainter objects. Although the individual positions in a group of several stars could usually be decoded unambiguously by inspection from deconvolved scans of the two orthogonal coordinates, another mathematical process would be needed to reconstruct a complicated two-dimensional continuous source. Each coordinate scan is a projection of the two-dimensional distribution onto that coordinate. A tomographic analysis of scans at a series of scan angles should provide a full image reconstruction in the general case of a continuous source intensity distribution, over a square somewhat smaller than the 5×5 arcsec FGS aperture.

Further development of deconvolution techniques might also be useful for other types of interferometry. Wherever complicated fringe shapes are formed from double, multiple, or continuous sources, it should be helpful to have direct solutions for the source distributions.

Thanks are due to several staff members at STScI: to Wayne Baggett for many helpful discussions throughout this work, to Wayne Baggett, Larry Taff, and Glenn Schneider for critical readings of the manuscript with many helpful suggestions, and to P. Bely, B. Bucciarelli, S. T. Holfeltz, and M. G. Lattanzi for support of various kinds.

REFERENCES

Franz, O. G. et al. 1991, ApJ, 377, L17

Franz, O. G., Wasserman, L. H., Nelan, E., Lattanzi, M. G., Bucciarelli, B., and Taff, L. G. 1992, AJ, 103, 190

FGS Instrument Team, 1992, Hubble Space Telescope Fine Guidance Sensors Instrument Handbook (Baltimore, Space Telescope Science Institute)

Press, W. H., Flannery, B. P., Teukolsky, S. A., and Veterling, W. T. 1986, Numerical Recipes (Cambridge, Cambridge University Press)